

Phase diagram of spin 1 antiferromagnetic Bose-Einstein condensates

David Jacob, Lingxuan Shao, Vincent Corre, Tilman Zibold, Luigi

De Sarlo, Emmanuel Mimoun, Jean Dalibard and Fabrice Gerbier

Laboratoire Kastler Brossel, CNRS, ENS, UPMC, 24 rue Lhomond, 75005 Paris

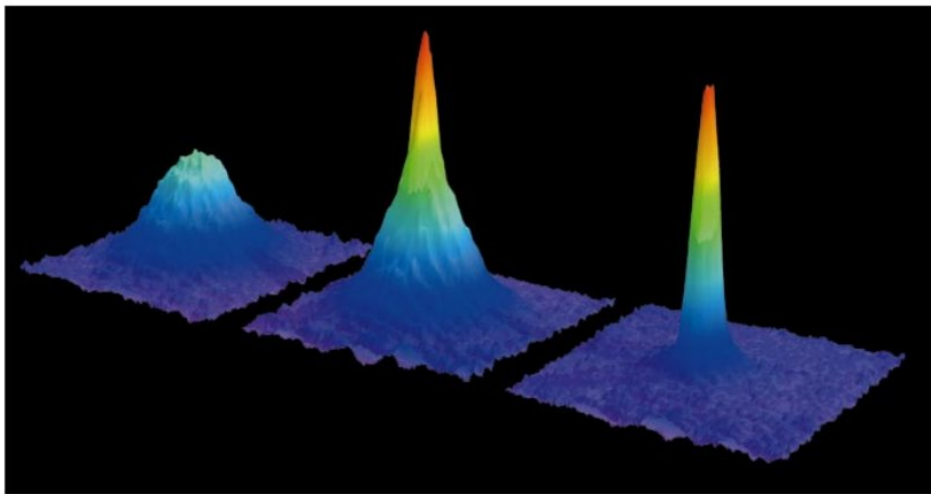
(Dated: September 13, 2012)

We study experimentally the equilibrium phase diagram of a spin 1 Bose-Einstein condensate with antiferromagnetic interactions, in a regime where spin and spatial degrees of freedom are decoupled. For a given total magnetization m_z , we observe for low magnetic fields an “antiferromagnetic” phase where atoms condense in the $m = \pm 1$ Zeeman states, and occupation of the $m = 0$ state is suppressed. Conversely, for large enough magnetic fields, a phase transition to a “broken axisymmetry” phase takes place: The $m = 0$ component becomes populated and rises sharply above a critical field $B_c(m_z)$. This behavior results from the competition between antiferromagnetic spin-dependent interactions (dominant at low fields) and the quadratic Zeeman energy (dominant at large fields). We compare the measured B_c as well as the global shape of the phase diagram with mean-field theory, and find good quantitative agreement.

Overview

- Examine a quantum liquid with spin \rightarrow Spinor Condensates
- Competition between spin-dependent interactions and quadratic Zeeman effect drives a quantum phase transition
- Compare the measurements with mean-field theory

First Realization of a Bose-Einstein Condensate



Spinor Condensates

Ultracold atoms in 2. Quantization:

$$\hat{H} = \int d^3\vec{x} \hat{\psi}^\dagger(\vec{x}) \left(-\frac{\hbar^2}{2m} \nabla^2 + V(\vec{x}) \right) \hat{\psi}(\vec{x}) \\ + \frac{1}{2} \frac{4\pi a_s \hbar^2}{m} \int d^3x \hat{\psi}^\dagger(\vec{x}) \hat{\psi}^\dagger(\vec{x}) \hat{\psi}(\vec{x}) \hat{\psi}(\vec{x})$$

- V is the trapping potential
- only s-wave scattering and contact interactions

Now spin carrying atoms are trapped by purely optical means:

$$\hat{H} = \int d^3r \left\{ \hat{\psi}_m^\dagger \left(-\frac{\hbar^2}{2m} \nabla^2 + V_{\text{ext}} \right) \hat{\psi}_m + \frac{g_{ij,kl}}{2} \hat{\psi}_i^\dagger \hat{\psi}_j^\dagger \hat{\psi}_k \hat{\psi}_l \right\}$$

Spinor Condensates

Interactions are rotationally symmetric \Rightarrow Spin is conserved

$$\hat{V}(r_1, r_2) = \sum_{S=0,2} g_S \hat{P}_S \delta(r_1 - r_2),$$

where $g_S = \frac{4\pi\hbar^2 a_S}{m}$

Rewrite the interaction potential in terms of spin operators:

$$\begin{aligned}(\mathbf{F}_1 \cdot \mathbf{F}_2)|\phi\rangle &= (\mathbf{F}_1 \cdot \mathbf{F}_2)(\hat{P}_0 + \hat{P}_2)|\phi\rangle \\ &= \frac{1}{2} [(\mathbf{F}_1 + \mathbf{F}_2)^2 - \mathbf{F}_1^2 - \mathbf{F}_2^2] (\hat{P}_0 + \hat{P}_2)|\phi\rangle \\ &= (-2\hat{P}_0 + \hat{P}_2)|\phi\rangle,\end{aligned}$$

$$\Rightarrow \hat{V}(r_1, r_2) = \left(\frac{g_0 + 2g_2}{3} + \frac{g_2 - g_0}{3} \mathbf{F}_1 \cdot \mathbf{F}_2 \right) \delta(r_1 - r_2).$$

Spinor Condensates

Write down the interaction terms in detail:

$$c_0 \hat{\psi}_m^\dagger \hat{\psi}_j^\dagger \hat{\psi}_j \hat{\psi}_m + c_2 \hat{\psi}_m^\dagger (F_\nu)_{mj} \hat{\psi}_j \cdot \hat{\psi}_l^\dagger (F_\nu)_{lk} \hat{\psi}_k =$$

$$(c_0 + c_2) \hat{\psi}_1^\dagger \hat{\psi}_1^\dagger \hat{\psi}_1 \hat{\psi}_1 + c_0 \hat{\psi}_0^\dagger \hat{\psi}_0^\dagger \hat{\psi}_0 \hat{\psi}_0 + (c_0 + c_2) \hat{\psi}_{-1}^\dagger \hat{\psi}_{-1}^\dagger \hat{\psi}_{-1} \hat{\psi}_{-1}$$

$$+ 2(c_0 + c_2) \hat{\psi}_1^\dagger \hat{\psi}_0^\dagger \hat{\psi}_1 \hat{\psi}_0 + 2(c_0 + c_2) \hat{\psi}_{-1}^\dagger \hat{\psi}_0^\dagger \hat{\psi}_{-1} \hat{\psi}_0 + 2(c_0 - c_2) \hat{\psi}_1^\dagger \hat{\psi}_{-1}^\dagger \hat{\psi}_1 \hat{\psi}_{-1}$$

$$+ 2c_2 \hat{\psi}_0^\dagger \hat{\psi}_0^\dagger \hat{\psi}_1 \hat{\psi}_{-1} + 2c_2 \hat{\psi}_1^\dagger \hat{\psi}_{-1}^\dagger \hat{\psi}_0 \hat{\psi}_0.$$

- three self-scattering terms
- three cross-scattering terms
- two spin relaxation terms

Meanfield Ansatz

Plug in the expression for the contact interaction:

$$\hat{H} = \int d^3r \left[\hat{\psi}_m^\dagger \left(-\frac{\hbar^2}{2M} \nabla^2 + V_{\text{ext}} \right) \hat{\psi}_m + \frac{c_0}{2} \hat{\psi}_m^\dagger \hat{\psi}_j^\dagger \hat{\psi}_j \hat{\psi}_m \right. \\ \left. + \frac{c_2}{2} \hat{\psi}_m^\dagger (F_\nu)_{mj} \hat{\psi}_j \cdot \hat{\psi}_l^\dagger (F_\nu)_{lk} \hat{\psi}_k \right],$$

Use $\hat{\psi} = \sqrt{n} \vec{\xi}$ (where $|\vec{\xi}|^2 = 1$ and n is the atomic density)

$$E[\{\phi_i\}] = \int d^3r \left\{ \frac{\hbar^2}{2m} (\nabla \sqrt{n})^2 + \frac{\hbar^2}{2m} (\nabla \vec{\xi})^2 n + (V_{\text{ext}} - \mu) \right. \\ \left. + \frac{n^2}{2} (c_0 + c_2 \langle \vec{F} \rangle^2) \right\}$$

where $\langle \vec{F} \rangle = \sum_{kl} \xi_k^* \vec{F}_{kl} \xi_l$

Detection of Different Hyperfine Components

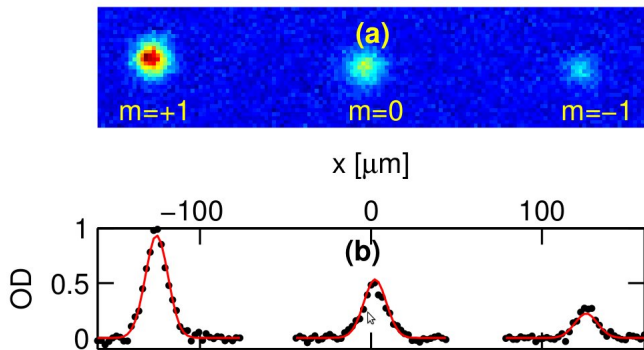
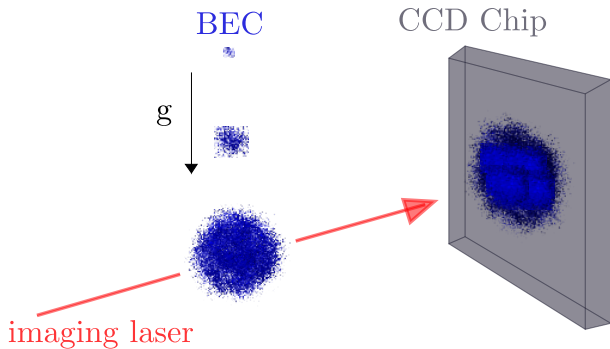


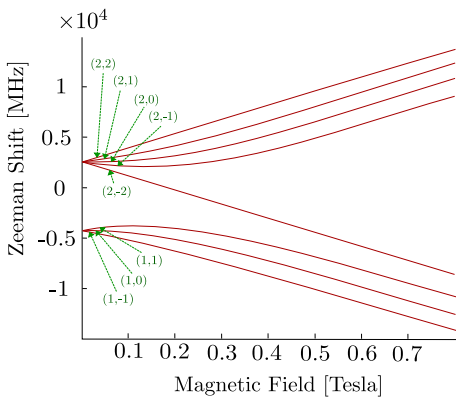
FIG. 1: (Color online) **a**: Absorption image of a spin 1 BEC after expansion in a magnetic gradient. **b**: Horizontal cuts through the images in (a). The same function (shown by straight lines), only recentered and reweighted, is used to fit the density profile of each Zeeman state.

Time-of-Flight Imaging

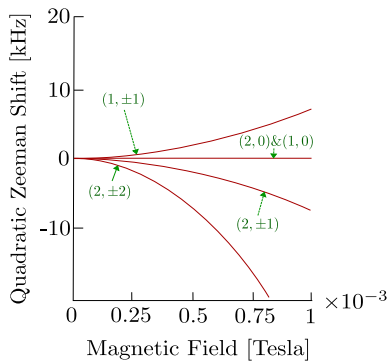


Effects of Magnetic Fields

(a)



(b)



Effects of Magnetic Fields

$$E[\{\phi_i\}] = H_S + \frac{c_2}{2} \langle \vec{F} \rangle^2 - p \langle F_z \rangle + q \langle F_z^2 \rangle$$

where $p = p_0 B$ and $q = q_0 B^2$

Express this in terms of occupancies of the hyperfine components:

$$\begin{aligned} \frac{E[\{n_i\}]}{N} &= \frac{H_S}{N} + \frac{c_2 n}{2} \left((n_1 - n_{-1})^2 + 2n_0 (\sqrt{n_1} \pm \sqrt{n_{-1}}) \right) \\ &- p(n_1 - n_{-1}) + q(n_1 + n_{-1}) \end{aligned}$$

Minimize this energy functional under the constraints:

- Particle number N is conserved $\Rightarrow n_1 + n_0 + n_{-1} = 1$
- Magnetization $m = n_1 - n_{-1}$ is conserved

Effects of Magnetic Fields

Minimize

$$\mathcal{F}(x) = c_2 n \left(x - \sqrt{x^2 - m^2} \right) (1 - x) + q x$$

where $x = n_1 + n_{-1}$

Introduce $q_c = c_2 n \left(1 - \sqrt{1 - m^2} \right)$

- For $q < q_c$: $x_0 = 1 \Leftrightarrow n_0 = 0 \Rightarrow$ Antiferromagnetic Phase
- For $q > q_c$: $x_0 < 1$ & $n_0 \neq 0 \Rightarrow$ Broken Axisymmetry Phase

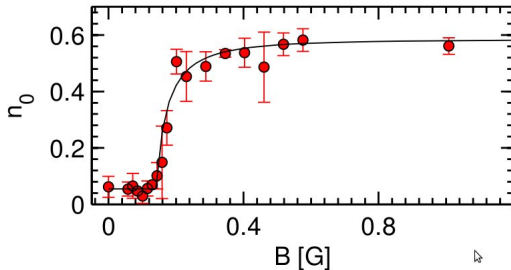


FIG. 2: (Color online) Sample data showing the population n_0 of the $m = 0$ Zeeman state versus applied magnetic field B , for a magnetization $m_z \approx 0.4$. The solid line is a fit to the data using Eq. (5). Vertical error bars show statistical uncertainties on the measured values (one standard deviation).

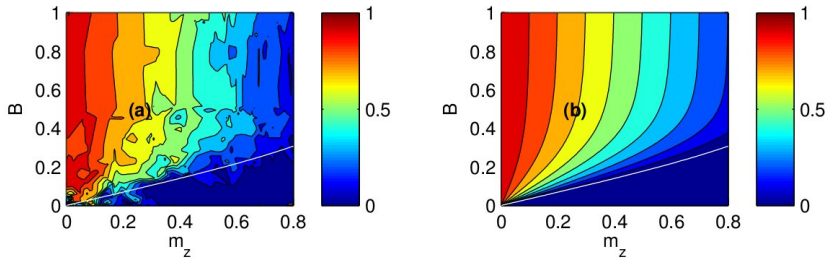


FIG. 3: (Color online) **a**: Experimental phase diagram showing the population n_0 of the $m = 0$ Zeeman state versus magnetization m_z and applied magnetic field B . The plot shows a contour interpolation through all data points, with magnetization ranging from 0 to 0.8. The white line is the predicted critical field B_c separating the two phases, deduced from Eq. (4) by $q_c = q_B B_c^2$. **b**: Theoretical prediction for n_0 at $T = 0$ K.

Summary

- "We explored experimentally the phase diagram of spin 1 BECs with antiferromagnetic interactions"
- "Two phases are found, reflecting the competition between the spin-dependent interactions and the quadratic Zeeman energy"
- "The measurements are in quantitative agreement with mean-field theory"

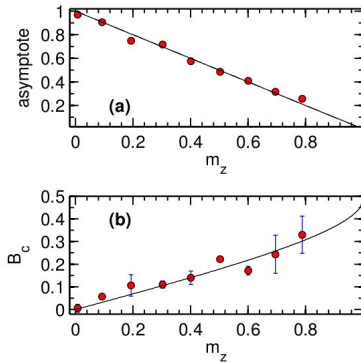


FIG. 4: (Color online) **a**: Asymptotic value of n_0 for large q (determined from $A_0 + A_1$ in Eq. 5). The solid line shows the value $1 - m_z$ expected at zero temperature. **b**: Measured critical field B_c versus magnetization. The solid line shows the values expected from Eq. (4) and $q_c = q_B B_c^2$, using $U_s/h \approx 65.6$ Hz. The gray area shows the uncertainty on the theoretical value of B_c , dominated by the 15% uncertainty on the spin-dependent scattering length a_s . For both plots, vertical error bars show statistical uncertainties on the measured values (one standard deviation).

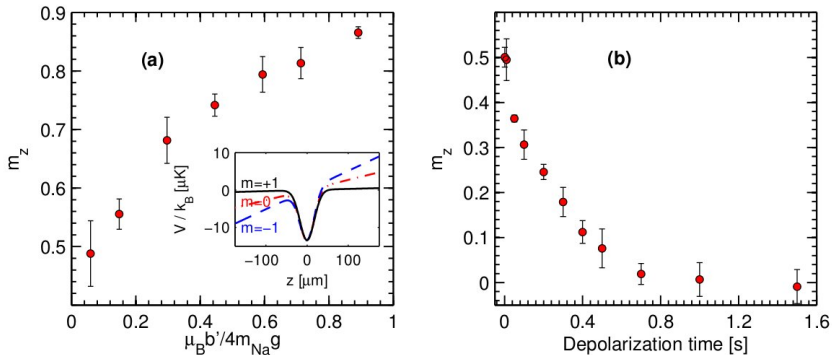


FIG. 5: **Supplementary Material-** (Color online) **(a)**: Spin distillation to prepare samples with high magnetization ($m_z > 0.5$). The plot shows the magnetization measured for cold clouds, as a function of the magnetic gradient b' in units of $m_{\text{Na}} g / \mu_B$, with g the acceleration of gravity and μ_B the Bohr magneton. The inset shows a sketch of the potential energies for each Zeeman state along the vertical axis z . The potential drop is exaggerated for clarity, and is smaller than depicted in the actual experiment. **(b)**: Depolarization to prepare samples with low magnetizations ($m_z < 0.5$). The time shown corresponds to the length of a radio-frequency pulse at the Larmor frequency.